Power-Domain Non-Orthogonal Multiple Access Based Full-Duplex One-Way Wireless Relaying Network

Volkan Ozduran, Nurul Huda Mahmood and Hatim Chergui

Abstract

This study investigates power-domain non-orthogonal multiple access based wireless information exchange process. The investigation considers a dual-hop non-regenerative full-duplex wireless one-way relaying networks in the system model, where the source terminal transmits two different types of information and subtracts the interference signal at the destination by using successive interference cancellation technique. The outage probability, error probability, achievable rate, and ergodic rate of the considered system is analytically derived. In addition, optimum power allocation coefficients and relay terminal position are determined using the optimization techniques. Monte-Carlo simulation results validate the analytical and asymptotic derivations. The derived analytical expressions are found closely in agreement with the system level numerical results.

Index Terms

Cooperative communications, full-duplex, power-domain non-orthogonal multiple access.

I. Introduction

In recent years, higher capacity/throughput is required for many emerging applications. Within this scope, novel strategies like non-orthogonal multiple access (NOMA) and full-duplex (FD) techniques are proposed solutions to meet this challenge. The NOMA technique achieves better performance and provides spectral efficiency in comparison to the existing orthogonal multiple access (OMA) techniques in the literature [1]. This is because the NOMA strategy utilizes the power domain for the multiple access (MA), as opposed to OMA strategies which depend on orthogonalization in time/frequency/code domain [1]. FD communication, where a transceiver can simultaneously transmit and receive at the same time frequency slot, has also been proposed as a solution for improving the spectral efficiency [2].

The literature contains several types of studies coexisting of these techniques. The key references can be summarized as follows: Reference [3] provides a broad perspective regarding the application of the FD NOMA transmission in wireless cellular, relay, and cognitive radio networks. [4] considers half-duplex (HD) and FD based cooperative NOMA system structure, where the base station (BS) communicates with far user with the help of a nearby user, which operates in HD and FD modes with decode-and-forward (DF) strategy. In addition, [4] investigates

V. Ozduran is with the Department of Electrical and Electronics Engineering, Istanbul University-Cerrahpasa, Istanbul, Turkey. N. H. Mahmood is with 6G Flagship, Centre for Wireless Communications, University of Oulu, Finland. H. Chergui is with Centre Tecnologic Telecomunicacions Catalunya (CTTC), Barcelona, Spain. This work is partially supported by the Academy of Finland 6Genesis Flagship program (grant no. 318927). Corresponding e-mail: *volkan@istanbul.edu.tr*.

the direct-link effects on such a system performance. Reference [5] considers that BS sends superimposed two different types of information to two different users, which are user 1 (U1) and user 2 (U2). [5] also considers that U1 is located nearby the BS and assists the information exchange process and act as a DF based FD relay. First, U1 decodes its own message by using the successive interference cancellation (SIC) technique and subtracts it and then forwards the remaining information to U2. Reference [6] extends [5] by assuming that the BS and U2 have a direct link. [6] also considers the maximum ratio combining (MRC) technique at U2. [7] considers that the BS directly communicates with U1. However, the BS needs DF based FD relay terminal's assistance to conducts information exchange with U2.

Reference [8] considers that a single source terminal conducts information exchange with N available destination terminals via amplify-and-forward (AF) based HD relaying. In addition, [8] considers Nakagami-m fading environment and imperfect channel state information (CSI) that is caused by channel estimation error. [9] considers that the source terminal sends the superimposed signal by using NOMA to the destination terminal with the help of DF based HD relaying. [10] considers that the BS conducts information exchange with three users in a cellular coverage area. Since the other two users are located at the edge of the cellular coverage area, one user, which is located close to the BS, acts as a DF based FD relay terminal.

Reference [11] extends [9] by assuming that the destination terminal also receives the superimposed signal from the first phase. [12] also considers a similar system model as [5]. Apart from [5], reference [12] assumes that the nearby user, which is close to the BS, acts as a compress-and-forward (CF) based FD relay terminal. In addition, [12] considers user scheduling and pairing strategies based on the proportional fair principle. [13] considers that FD based BS communicates with two users, source one (S_1) and source two (S_2), where S_2 is the stronger NOMA user and assists the information exchange by acting as DF based FD relay. In addition, S_1 is the weak NOMA user and combines the received signals from the BS and the S_2. [13] also provides achievable rate region analysis and considers various schemes that maximize the achievable rate. [14] considers a system model, where the BS conducts information exchange with a nearby user. In addition, the BS conducts information exchange with a second user, which is located outside of the cellular coverage area, with the help of a DF based HD relay terminal. [15] investigates user association and resource allocation in a multi-cell in-band full-duplex (IBFD)-enabled network, which operates in NOMA. In addition, [15] performs a comparative analysis of HD and FD modes, as well as OMA and NOMA strategies.

On the other hand, [16] considers that a single source terminal communicates with two destination terminals with the help of multiple AF and DF based HD relay terminals. In addition, [16] proposes a novel two-stage relay selection strategy, which is based on AF and DF modes. [17] considers conventional downlink cooperative scenario, where the BS conducts information exchange with two users with the help of a single AF based HD relay terminal. [17] also assumes that the BS directly communicates with a nearby user and need the relay terminal's assistance to communicate with the far user. [18] considers that two source terminals communicate with a single destination terminal with the aid of AF and DF based HD relay terminals. [18] considers hybrid DF and AF strategy, which is based on whether the relay terminal is able to successfully decode the information. In the former case, the AF strategy amplifies the information and forwards it to the destination terminal. [19] considers that multi-user terminals communicate with two destinations via N available AF based HD relaying. [19] also proposes an outage probability minimizing joint user and relay selection strategy for a NOMA based cooperative network. [20] investigates the partial relay selection process in cooperative NOMA based AF HD relaying system structure. [21] considers a downlink scenario, where a single BS conducts information exchange with M mobile users via a single AF based HD relaying. In addition, [21] considers Nakagami-m fading environment for the performance analysis.

Reference [22] considers downlink NOMA based AF and DF relaying system structure, where the BS communicates with N users with the help of a single HD relay terminal. [23] considers a downlink scenario, where a single BS communicates with two end users with/without the help of HD based AF one-way relay (OWR). In addition, [23] considers Nakagami-m fading environment for the performance analysis. Likewise, [24] also considers a downlink scenario, where a multiple antenna BS communicates with the multiple antenna destination terminal with the help of a single antenna HD based AF OWR. In addition, [24] takes into consideration the imperfect channel state information that is caused by channel estimation error and considers Nakagami-m fading environment and also performs antenna selection strategy. [25] considers an NOMA AF wireless relaying network, where a single antenna source terminal communicates with a single antenna K destinations via a multiple antenna HD based AF OWR. [25] considers joint power allocations and relay beamforming techniques to maximize the achievable rate at the destination. [26] characterizes the performance of cooperative relaying in interference-limited multihop networks, where nodes are equipped with multi-rate and continuous power control capabilities.

Reference [27] considers that BS makes information exchange with two-end users by means of AF/DF based FD relay terminal. [27] utilizes power-domain NOMA technique for the information exchange process and considers outage probability and ergodic rate metrics for the performance analysis. [28] investigates the system performance of DF based FD relay-assisted power-domain NOMA network. In addition, [28] takes into consideration in-phase and quadrature-phase imbalance and also imperfect SIC effects on the system performance. [29] investigates the system performance of HD/FD based relay-assisted uplink/downlink power-domain NOMA network. [30] investigates the system outage performance of incremental relaying based energy harvesting NOMA system. Moreover, [30] utilizes optimization techniques to determine the power allocation and power splitting factors. [31] investigates the performance of joint relay selection and power allocation strategies for energy harvesting cooperative NOMA network.

At first glance at the aforementioned studies, most of them consider different types of system models, which are uplink and downlink power/code-domain NOMA serving multiple users, and/or decoding process. Note that uplink and downlink user-decoding process have different successive interference cancellation (SIC) decoding processes, which are based on the mobile terminals' location and channel qualities etc. [32], [33]. Differently from the aforementioned studies, this paper considers that single mobile terminal makes multiple information exchange with a single destination terminal via relay-assisted power-domain non-orthogonal channels. The investigation utilizes SIC technique at destination and decode the received information based on the power allocation coefficients, which are allocated based on the user preferences. The details are presented as in the following folds:

- The investigation in this paper considers a dual-hop FD based AF OWR system structure. The proposed structure considers that source terminal transmits multiple information to the end-user by means of AF based

FD relay terminal. The aforementioned structure utilizes power-domain NOMA for the information exchange process. Since the relay terminal operates in AF mode, the relay terminal simply amplifies the received signal. Therefore, the SIC process is considered at the destination terminal. In addition, since the relay terminal has limited computational capability, the practical application area of such a system model could be in coverage constrained wireless sensor networks applications. A single source node or mobile terminal may request a multiple information from central node or BS. In addition, sensor node or mobile station may prioritize the requested information and decode accordingly.

- In an effort to measure the aforementioned system model's performance, this paper utilizes the most important performance metrics, which are the outage probability (OP), the achievable rate (AR), the ergodic rate (ER), the error probability (EP), throughput and as well as the asymptotic analysis and optimization. The performance metrics are analytically derived and verified with the help of the Monte-Carlo based intensive computer simulations and numerical analysis. The relay terminal's optimum location, optimum power allocation coefficients, and transmit powers are obtained by using the Lagrangian Multiplier technique to support the obtained results. Results reveal that the power allocation coefficient optimization have significant effect on the system performance and provides an equal opportunity for information exchange process.

A. *Organization and Notations*

Rest of the paper is organized as follows: The system model and related channel statistics are presented in Section II. The performance analysis results, which are based on both upper-bound and high signal-to-noise-ratio (SNR) regimes are presented in Section III. Numerical results are presented in Section IV. Lastly, the paper concludes in section V.

Notations: Probability density function (PDF) and cumulative distribution function (CDF) of a random variable (RV) h are presented as: $f_h(.)$ and $F_h(.)$, respectively. The operator $\mathbb{E}[.]$ stands for expectation, while Pr(.) denotes probability. $G_{p,q}^{m,n}[.]$ is the Meijer's G-function [34, Eq. (21)] and $H_{p,q}^{m,n}[.]$ is the Fox's H-function [35, Eq. (1.1.1)]. $G_{p,q:p_1,q_1:p_2,q_2}^{m,n:m_1,n_1:m_2,n_2}[.]$ is the extended generalized bi-variate Meijer's G-function [36, Eq. (13)] and $H_{p,q:p_1,q_1:p_2,q_2}^{m,n:m_1,n_1:m_2,n_2}[.]$ is the upper incomplete bi-variate Fox's H-function [37], [38]. $\Gamma(.)$ is the complete Gamma function [39, Eq. (8.310.1)] and $\Gamma(a, b)$ is the incomplete Gamma function [39, Eq. (8.350.2^{11})]. The superscript "up" represents the upper-bound. All log are base 2 unless stated otherwise. Note that variable list is presented in the Table 1.

II. System Model and Channel Statistics

Figure 1 depicts a dual-hop NOMA based FD wireless OWR network system structure. Here, S_1 conducts information exchange with S_2 via a single FD one-way wireless relay terminal. S_1 and S_2 do not have a direct-link because of poor line-of-sight. Each terminal has a single omni-directional antenna in such a system model. The channel impulse responses between $S_1 \longrightarrow$ relay and relay $\longrightarrow S_2$ are h and g, respectively, which are complex Gaussian RVs with zero mean and variances σ_h^2 and σ_g^2, respectively (i.e.$h \sim \mathcal{CN}\left(0, \sigma_h^2\right)$ and $g \sim \mathcal{CN}\left(0, \sigma_g^2\right)$). The variable a, $a \sim \mathcal{CN}\left(0, \sigma_a^2\right)$ is loop-back interference (LI) at the relay terminal. The LI occurs because the

TABLE I: Variable list.

Variable	Explanation
S_1	Source 1
S_2	Source 2
P_s	Transmit power of S_1
P_r	Transmit power of relay
P_s^*	Optimized transmit power of S_1
P_r^*	Optimized transmit power of relay
P_T	Total transmit power
h	Channel impulse response between $S_1 \rightarrow$ relay
g	Channel impulse response between relay $\rightarrow S_2$
a	Loop-back interference channel impulse response
σ_h^2	Variance of h
σ_g^2	Variance of g
σ_a^2	Variance of a
β_1 and β_2	Power allocation coefficients
x_1 and x_2	Transmit information
n_r	AWGN at relay
σ^2	Noise variance
G	Amplification factor
n_{S_2}	AWGN at S_2
γ_{th}	Threshold rate for FD case
γ_{th}^{HD}	Threshold rate for HD case
Ω_h, Ω_g, and Ω_a	Mean of $\lvert h\rvert^2$, $\lvert g\rvert^2$, and $\lvert a\rvert^2$, respectively.
d	Distance
v	Path-loss exponent
R	Target Rate in bps/Hz.

relay terminal receive and transmit the information at the same time. The amplitudes of all channels are assumed distributed according to Rayleigh distributions.

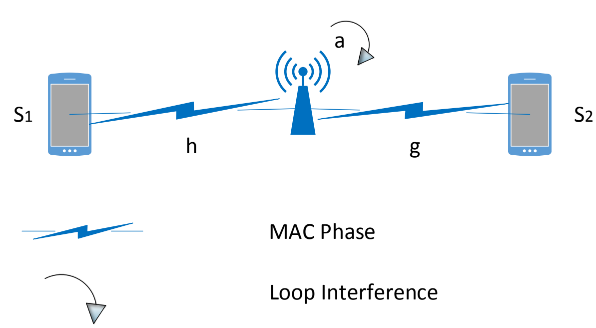

Fig. 1: A dual-hop non-orthogonal multiple access based full-duplex one-way wireless relaying network model.

The user S_1 intends to convey two messages, x_1 and x_2, to the destination S_2. Accordingly, S_1 transmits $\sqrt{\beta_1 P_s}x_1 + \sqrt{\beta_2 P_s}x_2$ to S_2 via a single FD OWR. Here, β_1 and β_2 are power allocation coefficients and can be formulated as: β_1+β_2=1 and $\beta_1 > \beta_2$. P_s represents S_1's transmit power. The symbols x_1, $\mathbb{E}[|x_1|^2] = 1$, and x_2, $\mathbb{E}[|x_2|^2] = 1$, represent the transmitted information. The received signal at the relay terminal can be written as

$$Z_r = h\left(\sqrt{\beta_1 \mathrm{P}_s} x_1 + \sqrt{\beta_2 \mathrm{P}_s} x_2\right) + \sqrt{\mathrm{P}_r} a + n_r \tag{1}$$

Here, P_r represents the relay terminal's transmit power. The variable $n_r \sim \mathcal{CN}\left(0, \sigma^2\right)$ is the additive white Gaussian noise (AWGN) at relay terminal. Since the relay terminal operates in AF mode, the amplification factor G can be calculated as

$$G = \sqrt{\frac{\mathrm{P}_r}{\mathrm{P}_s |h|^2 \left(\beta_1 + \beta_2\right) + \mathrm{P}_r |a|^2 + \sigma^2}} \tag{2}$$

The received signal at S_2 can be calculated as

$$Z_{S_2} = G\left(h\left(\sqrt{\beta_1 \mathrm{P}_s} x_1 + \sqrt{\beta_2 \mathrm{P}_s} x_2\right) + \sqrt{\mathrm{P}_r} a + n_r\right) g + n_{s_2} \tag{3}$$

where n_{S_2} is the AWGN at S_2. By using the SIC technique, which utilizes the decoding order: $\beta_1 > \beta_2$, for the signal separation process at the destination terminal, following expressions can be obtained at S_2

$$\mathrm{R}_{x_1} = \log\left(1 + \frac{G^2|h|^2|g|^2\beta_1 \mathrm{P}_s}{G^2|h|^2|g|^2\beta_2 \mathrm{P}_s + G^2|g|^2\mathrm{P}_r|a|^2 + G^2|g|^2\sigma^2 + \sigma^2}\right) \tag{4}$$

$$\mathrm{R}_{x_2} = \log\left(1 + \frac{G^2|h|^2|g|^2\beta_2 \mathrm{P}_s}{G^2|g|^2\mathrm{P}_r|a|^2 + G^2|g|^2\sigma^2 + \sigma^2}\right) \tag{5}$$

Substituting the G amplification factor into (4) and (5), R_{x_1} and R_{x_2} can be expressed as

$$\mathrm{R}_{x_1} = \log\left(1 + \underbrace{\frac{\frac{\gamma_x\gamma_y\beta_1}{[\gamma_a+1]}}{\frac{\gamma_x\gamma_y\beta_2+\gamma_x(\beta_1+\beta_2)+\gamma_y}{[\gamma_a+1]} + \gamma_y + 1}}_{\gamma_{x_1}}\right) \tag{6}$$

$$\mathrm{R}_{x_2} = \log\left(1 + \underbrace{\frac{\frac{\gamma_x\gamma_y\beta_2}{[\gamma_a+1]}}{\gamma_y + \frac{\gamma_x(\beta_1+\beta_2)+\gamma_y}{[\gamma_a+1]} + 1}}_{\gamma_{x_2}}\right) \tag{7}$$

where $\gamma_x = \frac{\mathrm{P}_s|h|^2}{\sigma^2}$, $\gamma_y = \frac{\mathrm{P}_r|g|^2}{\sigma^2}$, and $\gamma_a = \frac{\mathrm{P}_r|a|^2}{\sigma^2}$.

III. Performance Analysis

Performance metrics' analytical derivations are presented in this section. The OP, EP, AR, ER, and throughput performance metrics are considered for the performance analysis. This section also analyses the performance trend in the high SNR regime to provide further details on the asymptotic performance behavior.

A. Outage Probability

The OP is defined as the probability that the achievable rate cannot support the predefined target rate, which is R in bps/Hz. This process can also be formulated as: $\mathrm{P}_r[R_{x_i} \leq R]$. Analytically speaking, utilizing the logarithm properties, the OP is the CDF of received SNR/signal-to-interference plus noise ratio (SINR) evaluated at the target threshold rate, γ_{th} [40].

Given the intractable form of γ_{x_1} and γ_{x_2} in (6) and (7), these expressions can be upper-bounded as

$$\begin{aligned}\gamma_{x_1} &= \frac{\gamma_x \gamma_y \beta_1}{\gamma_y\left(\gamma_x \beta_2 + \gamma_A + 1\right) + \gamma_x\left(\beta_1 + \beta_2\right)} \\ &= \frac{\frac{\gamma_x \gamma_y \beta_1}{\left(\gamma_x \beta_2 + \gamma_A + 1\right)\left(\beta_1 + \beta_2\right)}}{\frac{\gamma_y}{\left(\beta_1 + \beta_2\right)} + \frac{\gamma_x}{\left(\gamma_x \beta_2 + \gamma_A + 1\right)}} \\ &= \beta_1 \frac{AB}{A+B} \leq \gamma_{x_1}^{\mathrm{up}} = \beta_1 \min\left(\mathrm{A}, \mathrm{B}\right) \end{aligned} \tag{8}$$

$$\begin{aligned}\gamma_{x_2} &= \frac{\gamma_x \gamma_y \beta_2}{\gamma_y\left(\gamma_A + 1\right) + \gamma_x\left(\beta_1 + \beta_2\right)} = \frac{\frac{\gamma_x \gamma_y \beta_2}{\left(\gamma_A + 1\right)\left(\beta_1 + \beta_2\right)}}{\frac{\gamma_y}{\left(\beta_1 + \beta_2\right)} + \frac{\gamma_x}{\left(\gamma_A + 1\right)}} \\ &= \beta_2 \frac{AC}{A+C} \leq \gamma_{x_2}^{\mathrm{up}} = \beta_2 \min\left(\mathrm{A}, \mathrm{C}\right) \end{aligned} \tag{9}$$

where $\gamma_A = \gamma_a + 1$, $A = \frac{\gamma_y}{(\beta_1+\beta_2)}$, $B = \frac{\gamma_x}{(\gamma_x\beta_2+\gamma_A+1)}$ and $C = \frac{\gamma_x}{(\gamma_A+1)}$. The CDFs of $\gamma_{x_1}^{up}$ and $\gamma_{x_2}^{up}$ are given by the following proposition.

Proposition 1. *The $F_{\gamma_{x_1}}^{up}$ and $F_{\gamma_{x_2}}^{up}$ can be calculated as*

$$F_{\gamma_{\mathrm{x}_1}}^{\mathrm{up}}\left(\gamma_{\mathrm{th}}\right) = 1 - \left(\frac{1}{\mathrm{P}_r \Omega_a}\right)\left(\frac{\gamma_{\mathrm{th}}}{\left(\beta_1 - \gamma_{th}\beta_2\right)\mathrm{P}_s \Omega_h} + \frac{1}{\mathrm{P}_r \Omega_a}\right)^{-1} e^{-\gamma_{\mathrm{th}}\left(\frac{\beta_1+\beta_2}{\beta_1 \mathrm{P}_s \Omega_g} + \frac{2}{\left(\beta_1 - \gamma_{th}\beta_2\right)\mathrm{P}_s \Omega_h}\right)} \tag{10}$$

$$F_{\gamma_{\mathrm{x}_2}}^{\mathrm{up}}\left(\gamma_{\mathrm{th}}\right) = 1 - \left(\frac{1}{\mathrm{P}_r \Omega_a}\right)\left(\frac{\gamma_{\mathrm{th}}}{\beta_2 \mathrm{P}_s \Omega_h} + \frac{1}{\mathrm{P}_r \Omega_a}\right)^{-1} e^{-\gamma_{\mathrm{th}}\left(\frac{\beta_1+\beta_2}{\beta_2 \mathrm{P}_s \Omega_g} + \frac{2}{\beta_2 \mathrm{P}_s \Omega_h}\right)} \tag{11}$$

where Ω_h, Ω_g, and Ω_a are mean of $|h|^2$, $|g|^2$, and $|a|^2$, respectively.

Proof. See Appendix A. □

B. Achievable Rate

With the help of [41, Eq. (32)] and modifying it to the FD case, the AR expression can be written as

$$\mathrm{AR}^{\mathrm{up}} = \underbrace{\mathbb{E}\left(\log\left(1 + \gamma_{x_1}^{\mathrm{up}}\right)\right)}_{\mathrm{R}_{\mathrm{x}_1}^{\mathrm{up}}} + \underbrace{\mathbb{E}\left(\log\left(1 + \gamma_{x_2}^{\mathrm{up}}\right)\right)}_{\mathrm{R}_{\mathrm{x}_2}^{\mathrm{up}}} \tag{12}$$

where $R_{x_1}^{\mathrm{up}} = \frac{1}{\ln 2}\int_0^\infty \frac{1-\mathrm{F}_{\gamma_{\mathrm{x}_1}}^{\mathrm{up}}(\gamma_{\mathrm{th}})}{1+\gamma_{\mathrm{th}}} \mathrm{d}\gamma_{\mathrm{th}}$ and $R_{x_2}^{\mathrm{up}} = \frac{1}{\ln 2}\int_0^\infty \frac{1-\mathrm{F}_{\gamma_{\mathrm{x}_2}}^{\mathrm{up}}(\gamma_{\mathrm{th}})}{1+\gamma_{\mathrm{th}}} \mathrm{d}\gamma_{\mathrm{th}}$ [41, Eq. (38)]. Substituting $F_{\gamma_{\mathrm{x}_1}}^{\mathrm{up}}(\gamma_{\mathrm{th}})$, which is (10), into the above related integral expression, $R_{x_1}^{\mathrm{up}}$ can be obtained as

$$R_{x_1}^{\mathrm{up}} = \frac{1}{\ln 2}\int_0^\infty \mathrm{e}^{-\gamma_{\mathrm{th}}\left(\frac{\beta_1+\beta_2}{\beta_1 \mathrm{P_s}\Omega_\mathrm{g}} + \frac{2}{\left(\beta_1 - \gamma_{\mathrm{th}}\beta_2\right)\mathrm{P_s}\Omega_\mathrm{h}}\right)}\left(\frac{\mathrm{P_r}\Omega_\mathrm{a}}{\left(\beta_1 - \gamma_{\mathrm{th}}\beta_2\right)\mathrm{P_s}\Omega_\mathrm{h}}\gamma_{\mathrm{th}} + 1\right)^{-1}\left(1 + \gamma_{\mathrm{th}}\right)^{-1} \mathrm{d}\gamma_{\mathrm{th}} \tag{13}$$

The integral expression in (13) can be solved as in the following proposition.

Proposition 2. *The $R_{x_1}^{\mathrm{up}}$ can be calculated as*

$$R_{x_1}^{\mathrm{up}} = -\frac{\mathrm{e}^{\left(\frac{2\alpha_2}{\beta_2}-\frac{\beta_1}{\beta_2}\alpha_1\right)}}{\alpha_3 \ln 2}\left(1-\frac{\beta_2}{\alpha_3\beta_1}\right)^{-1}\frac{\beta_2^2}{\left(\beta_1+\beta_2\right)\alpha_1\beta_1}\sum_{\mathrm{k}=0}^{\infty}\frac{\left(\frac{2\alpha_2}{\beta_2}\right)^{\mathrm{k}}}{\mathrm{k}!}\mathrm{H}_{1,0:1,1:1,1}^{0,1:1,1:1,1}\left[\begin{array}{c|c|c} 0,1,1;-\frac{\alpha_1\beta_1}{\beta_2} & 1,1,0 & 0,1,0 \\ -,-,-;- & 1,1,0 & 0,1,0 \end{array}\right.$$
$$\left.\left(1-\frac{\beta_2}{\alpha_3\beta_1}\right)\frac{\beta_2}{\alpha_1\beta_1},\frac{\beta_2}{\left(\beta_1+\beta_2\right)\alpha_1}\right] \tag{14}$$

Proof. See Appendix B. □

Likewise, substituting $F_{\gamma_{x_2}}^{\mathrm{up}}\left(\gamma_{\mathrm{th}}\right)$, which is (11), into $R_{x_2}^{\mathrm{up}} = \frac{1}{\ln 2}\int_0^{\infty}\frac{1-\mathrm{F}_{\gamma_{x_2}}^{\mathrm{up}}\left(\gamma_{\mathrm{th}}\right)}{1+\gamma_{\mathrm{th}}}\mathrm{d}\gamma_{\mathrm{th}}$ and using [34, Eq. (10, 11)] and also solving the integral expression with the help of [36, Eq. (13)] and [42], the following expression can be obtained. Note that the α term is set to 1 in [36, Eq. (13)].

$$R_{x_2}^{\mathrm{up}} = \frac{1}{\ln 2}\left[\left(\frac{\beta_1+\beta_2}{\beta_2\mathrm{P_s}\Omega_\mathrm{g}}+\frac{2}{\beta_2\mathrm{P_s}\Omega_\mathrm{h}}\right)^{-1}\mathrm{G}_{1,0:1,1:1,1}^{1,0:1,1:1,1}\left(\begin{array}{c|c|c} 1 & 0 & 0 \\ - & 0 & 0 \end{array}\middle|\left(\frac{\mathrm{P_r}\Omega_\mathrm{a}}{\beta_2\mathrm{P_s}\Omega_\mathrm{h}}\right)\left(\frac{\beta_1+\beta_2}{\beta_2\mathrm{P_s}\Omega_\mathrm{g}}+\frac{2}{\beta_2\mathrm{P_s}\Omega_\mathrm{h}}\right)^{-1},\left(\frac{\beta_1+\beta_2}{\beta_2\mathrm{P_s}\Omega_\mathrm{g}}+\frac{2}{\beta_2\mathrm{P_s}\Omega_\mathrm{h}}\right)^{-1}\right]\right. \tag{15}$$

Substituting (14) and (15) into (12), the final AR^{up} expression can be obtained.

C. Error Probability

This subsection now focuses on the EP performance analysis of the considered system. This paper utilizes the CDF based EP expression [43, Eq. (25)], as shown in (16), for the analytical derivations.

$$\bar{P_e} = \frac{a}{2}\sqrt{\frac{b}{\pi}}\int_0^{\infty}\frac{\exp\left(-\mathrm{bx}\right)}{\sqrt{x}}F(x)dx \tag{16}$$

where $a = b = 1$ represents the binary phase shift keying (BPSK) and $a = b = 2$ represents the quadrature phase shift keying (QPSK) modulations. This paper considers the BPSK modulation for the performance analysis. Substituting (10) into (16) and using distributive properties, following expression can be obtained.

$$\bar{P_e}_{x_1}^{\mathrm{up}} = \frac{1}{2\sqrt{\pi}}\left[\int_0^{\infty}\gamma_{th}^{-\frac{1}{2}}\exp\left(-\gamma_{\mathrm{th}}\right)\mathrm{d}\gamma_{\mathrm{th}}-\int_0^{\infty}\gamma_{\mathrm{th}}^{-\frac{1}{2}}\left(\frac{\mathrm{P_r}\Omega_\mathrm{a}\gamma_{\mathrm{th}}}{\left(\beta_1-\gamma_{\mathrm{th}}\beta_2\right)\mathrm{P_s}\Omega_\mathrm{h}}+1\right)^{-1}\mathrm{e}^{-\gamma_{\mathrm{th}}\left(\frac{\beta_1+\beta_2}{\beta_1\mathrm{P_s}\Omega_\mathrm{g}}+\frac{2}{\left(\beta_1-\gamma_{\mathrm{th}}\beta_2\right)\mathrm{P_s}\Omega_\mathrm{h}}+1\right)}\mathrm{d}\gamma_{\mathrm{th}}\right] \tag{17}$$

The integral expression in (17) can be solved as in the following proposition.

Proposition 3. *The $\bar{P_e}_{x_1}^{\mathrm{up}}$ can be calculated as*

$$\bar{P_e}_{x_1}^{\mathrm{up}} = \frac{1}{2\sqrt{\pi}}\left[\sqrt{\pi}-\sqrt{\frac{\beta_1}{\beta_2}}\frac{\beta_2}{\alpha_3}\mathrm{e}^{\frac{2\alpha_2}{\beta_2}-\frac{\beta_1}{\beta_2}\left(1+\alpha_1\right)}\frac{1}{\sqrt{\pi}}\left(1-\frac{\beta_2}{\alpha_3}\right)^{-1}\left(\frac{\beta_1\left(\alpha_1+1\right)}{\beta_2}\right)^{-1}\sum_{\mathrm{k}=0}^{\infty}\frac{\left(\frac{2\alpha_2}{\beta_2}\right)^{\mathrm{k}}}{\mathrm{k}!}\right.$$
$$\left.\times H_{1,0:1,1:1,1}^{0,1:1,1:1,1}\left[\begin{array}{c|c|c} 0,1,1;-\frac{\beta_1\left(\alpha_1+1\right)}{\beta_2} & \frac{1}{2},1,0 & 1,1,0 \\ -,-,-;- & 0,1,0 & 1,1,0 \end{array}\middle|\frac{\beta_2}{\beta_1\left(\alpha_1+1\right)},\left(1-\frac{\beta_2}{\alpha_3}\right)\frac{\beta_2}{\beta_1\left(\alpha_1+1\right)}\right]\right] \tag{18}$$

Proof. See Appendix C. □

For the $\bar{P}_{e_{x_2}}^{\text{up}}$ derivation, substituting (11) into (16) and utilizing [34, Eq. (10, 11)] and also solving the integral expressions with the help of [39, Eq. (3.326.2^{10})] and [34, Eq. (21)], the $\bar{P}_{e_{x_2}}^{\text{up}}$ can be obtained as

$$\bar{P}_{e_{x_2}}^{\text{up}} = \frac{1}{2\sqrt{\pi}}\left[\sqrt{\pi} - \left(\frac{\mathrm{P}_r\Omega_a}{\beta_2 \mathrm{P}_s \Omega_h}\right)^{-\frac{1}{2}} G_{1,2}^{2,1}\left(\left(\frac{\beta_1+\beta_2}{\beta_2 \mathrm{P}_s \Omega_g} + \frac{2}{\beta_2 \mathrm{P}_s \Omega_h} + 1\right)\left(\frac{\mathrm{P}_r\Omega_a}{\beta_2 \mathrm{P}_s \Omega_h}\right)^{-1} \middle| \begin{matrix} \frac{1}{2} \\ 0, \frac{1}{2} \end{matrix}\right)\right] \tag{19}$$

Note that α term in [34, Eq. (21)] is set to $\frac{1}{2}$.

D. Throughput Analysis

This subsection investigates the throughput performance analysis of given system model structure in figure 1. Utilizing [44, Eq. (15(a))], the CDF based throughput performance metric can be formulated for x_1 and x_2 as

$$\tau_{x_i}^{\text{up}} = \gamma_{th}\left(1 - F_{x_i}^{\text{up}}(\gamma_{th})\right), \forall_i = 1, 2 \tag{20}$$

Substituting (10) and (11) into (20), the throughput analytical derivations can be obtained for x_1 and x_2.

E. Asymptotic Analysis

In an effort to give more details regarding the derived analytical expressions, this subsection provides the asymptotic analysis of the OP and the EP expressions, which are presented as follows

1) Outage Probability:

Considering the Taylor's series expansions, the $\exp(x)$ term approximates to $1+x$, $x \to 0$ [39]. Substituting this variable change in (10) and (11), the following expressions can be obtained

$$F_{\gamma_{x_1}}^{\text{up}(\infty)}(\gamma_{\text{th}}) = 1 - \left(\frac{1}{\mathrm{P}_r\Omega_a}\right)\left(\frac{\gamma_{\text{th}}}{(\beta_1 - \gamma_{th}\beta_2)\,\mathrm{P}_s\Omega_h} + \frac{1}{\mathrm{P}_r\Omega_a}\right)^{-1}\left(1 - \gamma_{\text{th}}\left(\frac{\beta_1+\beta_2}{\beta_1 \mathrm{P}_s\Omega_g} + \frac{2}{(\beta_1 - \gamma_{th}\beta_2)\,\mathrm{P}_s\Omega_h}\right)\right) \tag{21}$$

$$F_{\gamma_{x_2}}^{\text{up}(\infty)}(\gamma_{\text{th}}) = 1 - \left(\frac{1}{\mathrm{P}_r\Omega_a}\right)\left(\frac{\gamma_{\text{th}}}{\beta_1 \mathrm{P}_s\Omega_h} + \frac{1}{\mathrm{P}_r\Omega_a}\right)^{-1}\left(1 - \gamma_{\text{th}}\left(\frac{1}{\beta_1 \mathrm{P}_s\Omega_g} + \frac{2}{\beta_1 \mathrm{P}_s\Omega_h}\right)\right) \tag{22}$$

2) Error Probability: The asymptotic behaviors of the error probability performance of x_2 is presented in this subsection. The error probability performance of x_2, with the help of [45, Eq. (07.34.03.0723.01)], Meijer's G function in (19) can be written as

$$e^{\zeta}\sqrt{\pi}\Gamma\left(\frac{1}{2}, \zeta\right) \tag{23}$$

where $\zeta = \left(\frac{\beta_1+\beta_2}{\beta_2 \mathrm{P}_s\Omega_g} + \frac{2}{\beta_2 \mathrm{P}_s\Omega_h} + 1\right)\left(\frac{\mathrm{P}_r\Omega_a}{\beta_2 \mathrm{P}_s\Omega_h}\right)^{-1}$. Utilizing [45, Eq. (06.06.06.0014.01)], (23) can be written as: $\sqrt{\pi}\zeta^{-\frac{1}{2}}\left(1 + O\left(\frac{1}{\zeta}\right)\right)$, where O represents the higher order term.

IV. Optimization

This section provides the optimization problems of the given system model. Two different types of optimization problems are considered, which are presented below.

A. Relay Position Optimization under Fixed Resource Allocation

The optimum position of the relay terminal is presented in this subsection. Assuming that the normalized distances between $S_1 \rightarrow$ relay is d^v and relay $\rightarrow S_2$ is $(1-d)^v$. Here, v term is the path-loss exponent and takes values between 2-6. By setting $\Omega_h = \frac{1}{d^v}$ and $\Omega_g = \frac{1}{(1-d)^v}$ and also substituting these expressions into (21), following expressions can be obtained.

$$\begin{aligned} F_{\gamma_{x_1}}^{\mathrm{up}(\infty)}(\gamma_{\mathrm{th}}) &= 1 - \left(\frac{\mathrm{P}_r \Omega_a \gamma_{\mathrm{th}} d^v}{(\beta_1 - \gamma_{th}\beta_2)\,\mathrm{P}_s} + 1\right)^{-1} \left(1 - \gamma_{\mathrm{th}}\left(\frac{(\beta_1+\beta_2)(1-d)^v}{\beta_1 \mathrm{P}_s} + \frac{2d^v}{(\beta_1 - \gamma_{th}\beta_2)\,\mathrm{P}_s}\right)\right) \\ &= 1 - (A_1 d^v + 1)^{-1}\left(1 - (B_1(1-d)^v + C_1 d^v)\right) \end{aligned} \tag{24}$$

where $A_1 = \frac{\mathrm{P}_r \Omega_a \gamma_{\mathrm{th}}}{(\beta_1 - \gamma_{th}\beta_2)\mathrm{P}_s}$, $B_1 = \frac{(\beta_1+\beta_2)\gamma_{\mathrm{th}}}{\beta_1 \mathrm{P}_s}$ and $C_1 = \frac{2\gamma_{\mathrm{th}}}{(\beta_1 - \gamma_{th}\beta_2)\mathrm{P}_s}$. Differentiating (24) with respect to d and setting it to 0, following expression can be obtained.

$$\begin{aligned} &\frac{\partial \mathcal{L}\left(F_{\gamma_{x_1}}^{\mathrm{up}(\infty)}(\gamma_{\mathrm{th}})\right)}{\partial d} = (A_1 d^v + 1)^{-2}\, v d^{v-1} \\ &\times \left(1 - (B_1(1-d)^v + C_1 d^v)\right) \\ &+ (A_1 d^v + 1)^{-1}\left(-\left(v(1-d)^{v-1} + v d^{v-1}\right)\right) \end{aligned} \tag{25}$$

$$\Longrightarrow \left(v(1-d)^{v-1} + v d^{v-1}\right) = 0 \Longrightarrow d = \tfrac{1}{2}.$$

Following the similar procedures for $F_{\gamma_{X_2}}^{\mathrm{up}\infty}(\gamma_{\mathrm{th}})$, the optimum location of the relay terminal can be obtained as halfway between the source and the destination.

B. Resource Allocation Optimization under Fixed Relay Location

This subsection now focuses on minimizing the outage probabilities of x_1 and x_2. The optimization problem and its constraints can be written as

$$\begin{aligned} \underset{\gamma_{th}}{\text{minimize}} \quad & \mathrm{F}_{\gamma_{x_1}}^{\mathrm{up}(\infty)}(\gamma_{\mathrm{th}}) \text{ and } \mathrm{F}_{\gamma_{x_2}}^{\mathrm{up}(\infty)}(\gamma_{\mathrm{th}}) \\ \text{subject to} \quad & \mathrm{P}_s + \mathrm{P}_r = \mathrm{P}_T \text{ and } 0 < \mathrm{P}_s, \mathrm{P}_r \\ & \beta_1 + \beta_2 = 1 \text{ and } \beta_1 > \beta_2 \end{aligned} \tag{26}$$

By defining $a = \frac{\gamma_{th}}{\Omega_h}$ and $b = \frac{\gamma_{th}}{\Omega_g}$ and replacing in $F_{\gamma_{x_2}}^{\mathrm{up}\infty}(\gamma_{\mathrm{th}})$, the following expressions can be obtained. Where $\mathrm{P}_s = p_f \mathrm{P}_T$, $\mathrm{P}_r = \left(1 - p_f\right)\mathrm{P}_T$, $p_f \epsilon\,(0,1)$, $p_f = \beta_1 + \beta_2$. Substituting p_f term into P_s and P_r, following expressions can be obtained as: $\mathrm{P}_s = (\beta_1+\beta_2)\,\mathrm{P}_T$, $\mathrm{P}_r = (1-\beta_1-\beta_2)\,\mathrm{P}_T$. Where $0 < \beta_2 < \beta_1 < 1$ and $\mathrm{P}_T > 0$. By doing these variable changes, $F_{\gamma_{x_1}}^{\mathrm{up}(\infty)}(\gamma_{\mathrm{th}})$, (21) and $F_{\gamma_{x_2}}^{\mathrm{up}(\infty)}(\gamma_{\mathrm{th}})$, (22) can be re-written as

$$F_{\gamma_{x_1}}^{\mathrm{up}(\infty)}(\gamma_{\mathrm{th}}) = 1 - \left(\frac{(1-\beta_1-\beta_2)\,\mathrm{P}_T \Omega_a a}{(\beta_1 - \gamma_{th}\beta_2)(\beta_1+\beta_2)\,\mathrm{P}_T} + 1\right)^{-1}\left(1 - \left(\frac{b}{\beta_1 \mathrm{P}_T} + \frac{2a}{(\beta_1 - \gamma_{th}\beta_2)(\beta_1+\beta_2)\,\mathrm{P}_T}\right)\right) \tag{27}$$

$$F_{\gamma_{x_2}}^{\mathrm{up}(\infty)}(\gamma_{\mathrm{th}}) = 1 - \left(\frac{(1-\beta_1-\beta_2)\,\mathrm{P}_T \Omega_a}{\beta_2(\beta_1+\beta_2)\,\mathrm{P}_T} a + 1\right)^{-1}\left(1 - \left(\frac{b}{\beta_2 \mathrm{P}_T} + \frac{2a}{\beta_2(\beta_1+\beta_2)\,\mathrm{P}_T}\right)\right) \tag{28}$$

Utilizing the Lagrangian multipliers, the first order derivative of $F_{\gamma_{x_1}}^{\text{up}(\infty)}(\gamma_{\text{th}})$ expressions with respect to β_1 and β_2 can be, respectively, obtained as

$$\frac{\partial \mathcal{L}\left(F_{\gamma_{x_1}}^{\text{up}(\infty)}(\gamma_{\text{th}})\right)}{\partial \beta_1} = \left(b\left(\beta_1 \mathrm{P}_T\right)^{-2} \mathrm{P}_T + 2a\left((\beta_1 - \gamma_{th}\beta_2)(\beta_1 + \beta_2)\mathrm{P}_T\right)^{-2}\left(2\beta_1 \mathrm{P}_T + \beta_2 \mathrm{P}_T - \gamma_{th}\beta_2 \mathrm{P}_T\right)\right) \tag{29}$$

$$\frac{\partial \mathcal{L}\left(F_{\gamma_{x_1}}^{\text{up}(\infty)}(\gamma_{\text{th}})\right)}{\partial \beta_2} = \left(2a\left((\beta_1 - \gamma_{th}\beta_2)(\beta_1 + \beta_2)\mathrm{P}_T\right)^{-2}\left(\beta_1 \mathrm{P}_T - \gamma_{th}\beta_1 \mathrm{P}_T - 2\gamma_{th}\beta_2 \mathrm{P}_T\right)\right) \tag{30}$$

By setting (29) and (30) to zero $2\beta_1\mathrm{P}_T + \beta_2\mathrm{P}_T = 0$ and $-\gamma_{th}\beta_1\mathrm{P}_T - 2\gamma_{th}\beta_2\mathrm{P}_T = 0$ terms are obtained. By using these two equality, the $\beta_1 = 2\beta_2$ term can be obtained. Substituting into $\beta_1 + \beta_2 = 1$ yields $\beta_1 = \frac{2}{3}$ and $\beta_2 = \frac{1}{3}$. Likewise, following the similar procedures,

$$\frac{\partial \mathcal{L}\left(F_{\gamma_{x_2}}^{\text{up}(\infty)}(\gamma_{\text{th}})\right)}{\partial \beta_1} = 2a\left(\beta_1\beta_2\mathrm{P}_T + \beta_2^2\mathrm{P}_T\right)^{-2}\left(\beta_2\mathrm{P}_T\right) \tag{31}$$

$$\frac{\partial \mathcal{L}\left(F_{\gamma_{x_2}}^{\text{up}(\infty)}(\gamma_{\text{th}})\right)}{\partial \beta_2} = \left(b\left(\beta_2\mathrm{P}_T\right)^{-2}\mathrm{P}_T + 2a\left(\beta_2(\beta_1 + \beta_2)\mathrm{P}_T\right)^{-2}\left(\beta_1\mathrm{P}_T + 2\beta_2\mathrm{P}_T\right)\right) \tag{32}$$

In a similar way, by setting (32) to zero, $2\beta_2\mathrm{P}_T + \beta_1\mathrm{P}_T = 0$ term is obtained. By using this equality, the $\beta_1 = 2\beta_2$ term can be obtained. Substituting into $\beta_1 + \beta_2 = 1$ yields $\beta_1 = \frac{2}{3}$ and $\beta_2 = \frac{1}{3}$.

The optimum transmit powers of S_1, which is P_s, and relay terminal, which is P_r are investigated in this subsection. In this regard, considering only the constant part of $F_{\gamma_{x_1}}^{\text{up}(\infty)}(\gamma_{\text{th}})$ and $F_{\gamma_{x_2}}^{\text{up}\infty}(\gamma_{\text{th}})$, and doing variable change, which is $\mathrm{P}_r = \mathrm{P}_T - \mathrm{P}_s$, and also differentiating with respect to P_s, the following expression is obtained.

$$\begin{aligned}
\frac{\partial \mathcal{L}\left(F_{\gamma_{x_1}}^{\text{up}(\infty)}(\gamma_{\text{th}})\right)}{\partial \mathrm{P}_s} &= 1 - (\mathrm{P}_T - \mathrm{P}_s)\mathrm{P}_s^{-1} \\
&= (-1)\mathrm{P}_s^{-1} + (\mathrm{P}_T - \mathrm{P}_s)(-1)\mathrm{P}_s^{-2} \\
&= \mathrm{P}_s^* = \frac{\mathrm{P}_T}{2} \\
&= \mathrm{P}_r^* = \frac{\mathrm{P}_T}{2}
\end{aligned} \tag{33}$$

Considering the similar procedures and utilizing the $F_{\gamma_{x_2}}^{\text{up},\infty}(\gamma_{\text{th}})$, $\mathrm{P}_s^* = \frac{\mathrm{P}_T}{2}$ and $\mathrm{P}_r^* = \frac{\mathrm{P}_T}{2}$ terms can be obtained.

V. Numerical Results

Numerical results section verifies the theoretical analysis through Monte-Carlo simulations. The simulation parameters for optimized and non-optimized cases are presented in the Table 2. According to Table 2, the target rate is set to 1 bps/Hz. By using the logarithm properties, the target threshold rate, γ_{th}, is set to 1 bps/Hz. for the FD case and 3 bps/Hz. for the HD case. System total transmit power is set to P_T, which is equal to $\mathrm{P}_s + \mathrm{P}_r$. Regarding the optimized/non-optimized cases, S_1 and relay terminal's transmit powers are set to $\frac{\mathrm{P}_T}{2}$. The non-optimized case utilized as a benchmark and equally transmit power allocated. The optimized transmit powers are obtained according to (33). Regarding the power allocation coefficients, β_1+β_2=1 and $\beta_1 > \beta_2$, non-optimized β_1 and β_2 are set to $\frac{9}{10}$ and $\frac{1}{10}$, respectively. According to Section 4.2, the optimized power allocation coefficients are set to $\beta_1 = \frac{2}{3}$ and

$\beta_2 = \frac{1}{3}$. Regarding the LI variance, which is σ_a^2, $P_r^{\lambda-1}$, $0 \leq \lambda \leq 1$ [46] formulation is utilized. This is because, advances in signal processing and special antenna design techniques can minimize the LI effects. Therefore, the λ term is set to 0.2 for the optimized/non-optimized OP, ER, ASR, and throughput performance metric. The λ term is set to 0.57 for the optimized/non-optimized EP performance analysis. It is verified with the Monte-Carlo based intensive computer simulations that when the λ term is set to 0.57, analytical and simulation curves provide suitable results compared to 0.2 for EP performance analysis. Main channel variances, which are σ_h^2 and σ_g^2, are set to 1 for optimized/non-optimized cases.

TABLE II: Simulation parameters.

	Optimized	Non-Optimized
Target rate: R, in bps/Hz.	1 bps/Hz.	1 bps/Hz.
Target threshold rate for FD case: γ_{th}, in bps/Hz.	$2^R - 1$ bps/Hz.	$2^R - 1$ bps/Hz.
Target threshold rate for HD case: γ_{th}^{HD}, in bps/Hz.	$2^{2R} - 1$ bps/Hz.	$2^{2R} - 1$ bps/Hz.
Total transmit power: $P_T = P_s + P_r$	$P_s^* = \frac{P_T}{2}$, $P_r^* = \frac{P_T}{2}$	$P_s = \frac{P_T}{2}$, $P_r = \frac{P_T}{2}$
Power allocation coefficients: β_1 and β_2	$\beta_1 = \frac{2}{3}$ and $\beta_2 = \frac{1}{3}$	$\beta_1 = \frac{9}{10}$ and $\beta_2 = \frac{1}{10}$
The LI variance: σ_a^2	$P_r^{\lambda-1}$, $0 \leq \lambda \leq 1$ [46], λ=0.2 and 0.57	$P_r^{*\lambda-1}$, $0 \leq \lambda \leq 1$, $\lambda = 0.2$ and $\lambda = 0.57$
Main channel variances: σ_h^2 and σ_g^2	$\sigma_h^2 = 1$ and $\sigma_g^2 = 1$	$\sigma_h^2 = 1$ and $\sigma_g^2 = 1$

The outage probability performance comparisons of x_1 and x_2 are illustrated in figure 2. The target rate, R, is set to 1 bps/Hz. The LI variance, σ_a^2 is modeled as $P_r^{\lambda-1}$, where $0 \leq \lambda \leq 1$ [46]. To this end, the λ term is set to 0.2. For the non-optimized case, it is assumed that $P_s = P_r = \frac{P_T}{2}$ and $\beta_1 = \frac{9}{10}$, $\beta_2 = \frac{1}{10}$. Interpreting figure 2 based on these system setting configurations, in low and high SNR regimes, x_1 achieves better outage performance values than x_2, since it is transmitted with higher power. So as to achieve 10^{-3} outage performance, the required SNRs for x_1 and x_2 are between 35 dB-40 dB and 45 dB-50 dB, respectively. The obtained results are closely agreement with the analytical and asymptotic derivations, which are (10), (11) and (21), (22), respectively.

The optimized outage performance of x_1 and x_2 is presented in figure 3. According to (33), the optimum transmit powers are $P_s = \frac{P_T}{2}$ and $P_r = \frac{P_T}{2}$. In addition, according to (31) and (32), $\beta_1 = \frac{2}{3}$, $\beta_2 = \frac{1}{3}$. Based on these system model configurations, x_1's performance curves get worse and x_2's performance curves improves and both curves meet in an optimum level in figure 3. For instance, to achieve 10^{-3} outage performance, the required SNRs for optimized x_1 and x_2 are between 40dB-45dB. The obtained results are closely agreement with the analytical and asymptotic derivations, which are (10), (11) and (21), (22), respectively.

Figure 4 presents the non-optimized outage performance comparison of HD and FD cases for x_1 and x_2. The target rate, which is R, is set to 1 bps/Hz and the related target threshold rates are obtained as: 1 bps/Hz. and 3 bps/Hz. for FD and HD cases, respectively. The transmit powers and power allocation coefficients are set to $P_s = P_r = \frac{P_T}{2}$ and $\beta_1 = \frac{9}{10}$, $\beta_2 = \frac{1}{10}$, respectively. Interpreting the figure 4, so as to reach to 10^{-3} outage performance the required SNRs are 39 dB and 43 dB for FD and HD cases of x_1, respectively. Regarding the x_2 case, the required SNRs for

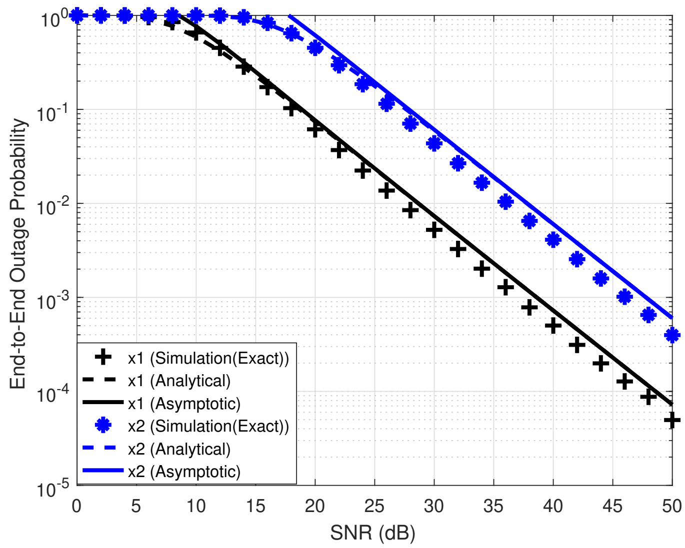

Fig. 2: The non-optimized outage probability performance comparisons of the x_1 and x_2.

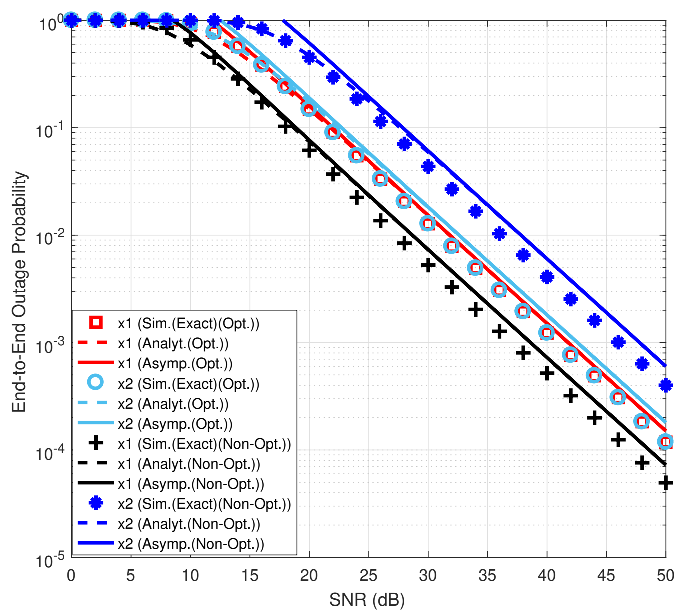

Fig. 3: The outage probability performance comparisons of optimized/non-optimized x_1 and x_2.

10^{-3} outage performance, 47 dB and 50 dB for FD and HD cases, respectively. Interpreting the obtained results, FD based x_1 and x_2 achieve better outage performance than HD counterpart. This observation occurs because of the pre-log factor differences, which affects the target threshold rate, and the minimized LI effects.

Figure 5 plots the optimized outage performance comparison of HD and FD cases for x_1 and x_2. Based on the optimization section, the transmit powers and power allocation coefficients are set to $\mathrm{P}_s = \mathrm{P}_r = \frac{\mathrm{P}_T}{2}$ and $\beta_1 = \frac{2}{3}$,

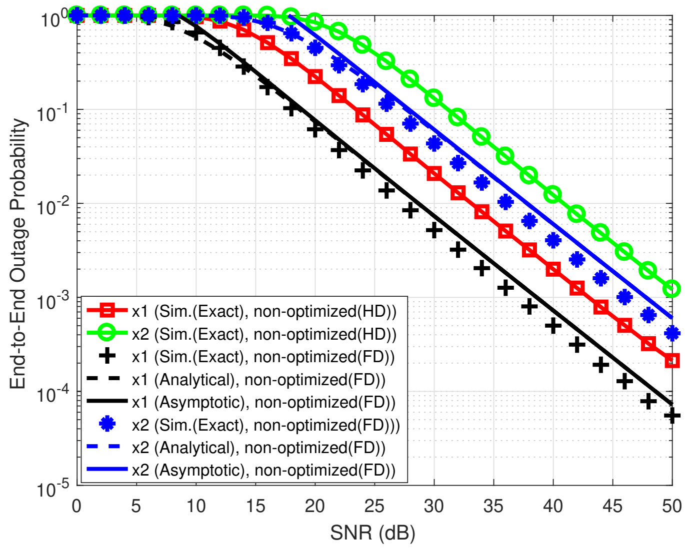

Fig. 4: The outage probability performance comparisons of non-optimized HD and FD x_1 and x_2.

$\beta_2 = \frac{1}{3}$, respectively. So as to achieve 10^{-3} outage performance, the FD based x_1 and x_2 meet between 40-45 dB. The HD based optimized x_2 reaches to 10^{-3} outage performance at 45 dB. However, the optimized HD based x_1 cannot support the pre-defined target rate and saturates along the SNR regimes.

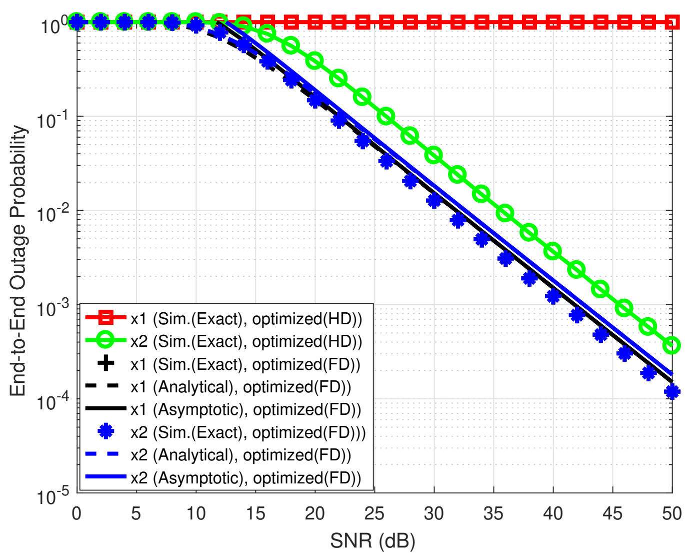

Fig. 5: The outage probability performance comparisons of optimized HD and FD x_1 and x_2.

Figure 6 plots the non-optimized error probability performance evaluations of x_1 and x_2, which utilizes $\beta_1 = \frac{9}{10}$ and $\beta_2 = \frac{1}{10}$. Note that the λ term is set to 0.57 in figure 6 implementation. According to figure 6, x_1 achieves better error probability performance values than x_2. For instance, to achieve 10^{-2} error performance, the required SNRs for x_1 and x_2 are between 25dB-30dB and 30dB-35dB, respectively. The obtained results are closely agreement with the analytical and asymptotic derivations, which are (18), (19), and (23).

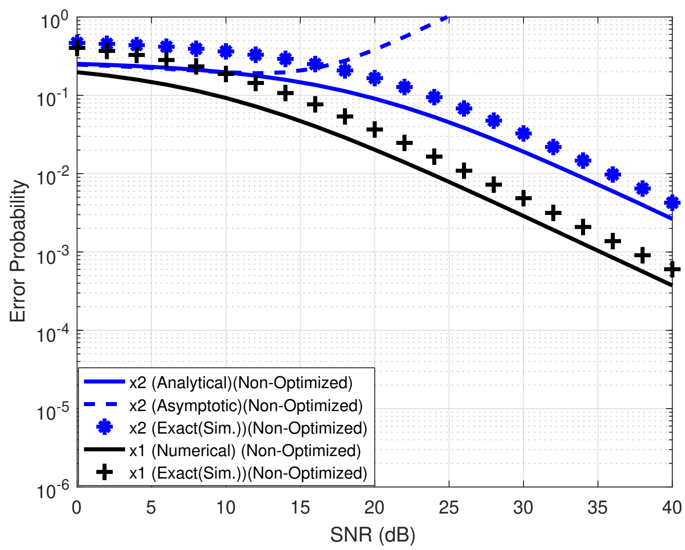

Fig. 6: The non-optimized error probability performance comparisons of x_1 and x_2.

Figure 7 presents the error probability performance evaluation of the x_1 and x_2 with the optimized power allocation coefficients, which are $\beta_1 = \frac{2}{3}$ and $\beta_2 = \frac{1}{3}$. In low SNR regimes, the optimized x_1 and x_2 achieves a similar error probability performance and meet in a common line. For instance to achieve 10^{-1} error probability performance the required SNR values 16 dB for the optimized x_1 and x_2 while it is 14 dB and 22 dB for the non-optimized x_1 and x_2, respectively. In other words, the optimization decreases the x_1's performance and improves the x_2's performance. In high SNR regimes, the x_1 diverges from the x_2 and saturates. The obtained results are closely agreement with the analytical and asymptotic derivations, which are (18), (19), and (23).

Figure 8 depicts the achievable ergodic rate and sum-rate performance evaluations. In reference to figure 8, in low SNR regimes, the ergodic rate of x_1 provides slightly better performance than the ergodic rate of x_2. However, in high SNR regimes, x_1's performance cannot be improved and saturates, while x_2's performance improves and provides better performance results. The saturation occurs because of the SIC process. The denominator of the R_{x_1}, which is (4), has the x_2's information, which acts as co-channel interference for x_1, while the denominator of the R_{x_2} does not have x_1's information. On the other hand, the achievable sum-rate provides better performance results than individual ergodic rate performance. The obtained results are closely agreement with the analytical derivations of (14) and (15).

The achievable ergodic rate and sum-rate performance evaluations with the optimized power allocation coefficients, which are $\beta_1 = \frac{2}{3}$ and $\beta_2 = \frac{1}{3}$ are presented in figure 9. Interpreting figure 9, the optimized power allocation coefficients do not effect the achievable sum-rate performance. This is because the total power allocation coefficient is equal to 1 in both cases. However, the optimized power allocation coefficients effect the ergodic rate performance

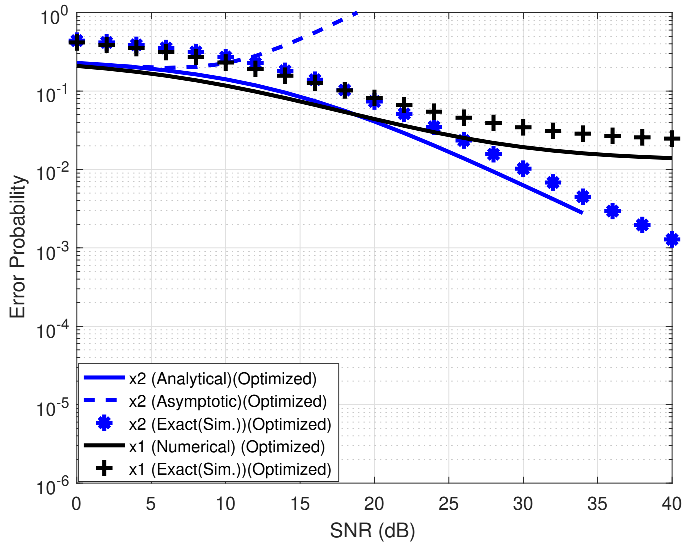

Fig. 7: The optimized EP performance comparisons of x_1 and x_2.

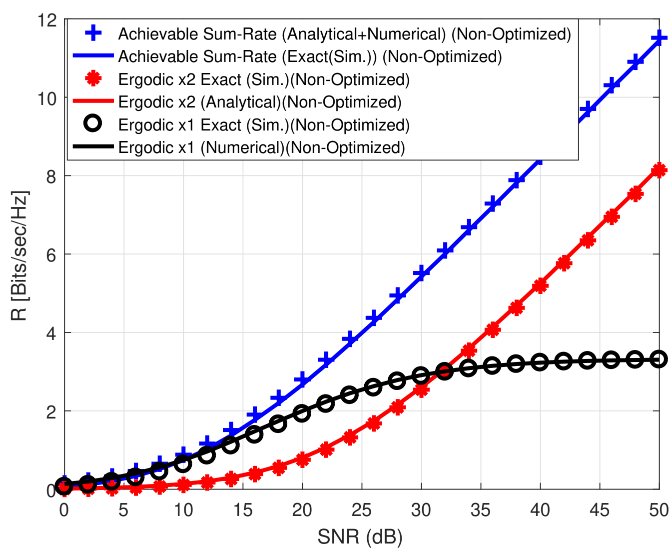

Fig. 8: The non-optimized achievable sum-rate and ergodic rate performance comparisons of x_1 and x_2.

of x_1 and x_2. For instance, to achieve 4 bps/Hz the required SNRs are 30 dB and 35 dB for the optimized and non-optimized ergodic rate of x_2, respectively. Regarding the ergodic rate of x_1, the optimized power allocation coefficients decreases the x_1's performance. For instance, the overall performance of ergodic rate of x_1 between 0-2 bps/Hz. while it is between 0-4 bps/Hz. in the non-optimized case. The obtained results are closely agreement with the analytical derivations of (14) and (15).

Figure 10 presents the optimized with respect to power allocation coefficients and non-optimized throughput

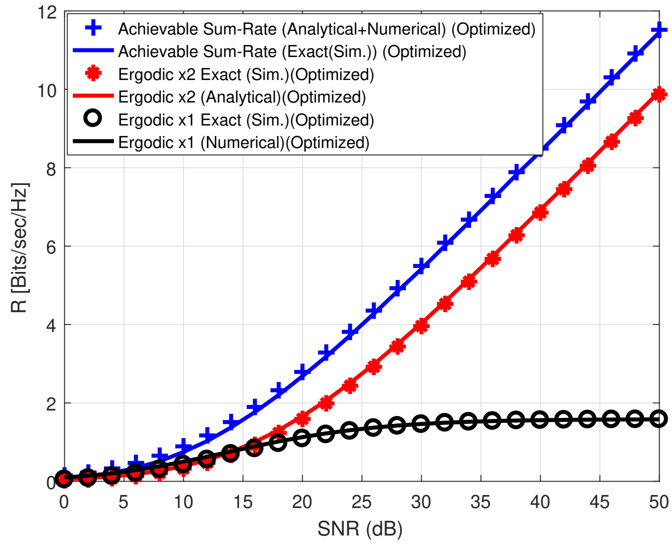

Fig. 9: The optimized achievable sum-rate and ergodic rate performance comparisons of x_1 and x_2.

performance comparison of x_1 and x_2. In reference to figure 10, the non-optimized x_1 achieves better throughput performance than the non-optimized x_2. This is because the power allocation coefficient factor differences, which are $\beta_1 = \frac{9}{10}$ and $\beta_2 = \frac{1}{10}$. The optimized power allocation coefficients minimize the throughput performance gap of x_1 and x_2. In other words, the optimized power allocation coefficients provide fair throughput rate for successful message delivery of x_1 and x_2. For instance to achieve 0.5 bps/Hz. throughput performance, the required SNR values are 10 dB and 20 dB for non-optimized x_1 and x_2, respectively. However, for the same throughput performance, the required SNR value is 15 dB for the optimized x_1 and x_2. The obtained results are closely agreement with the derived analytical expressions.

VI. Conclusions

Performance evaluations of the power-domain NOMA based wireless information exchange process have investigated in this study. The investigation has considered a dual-hop FD one-way wireless relaying network. The investigation has also considered that the transmitter transmits superimposed two different types of information to the destination terminal. This is a reasonable system model configuration. This is because a single source node or mobile terminal may request a multiple information from central node or BS. Sensor node or mobile station may prioritize the requested information and decode accordingly. Since the relay terminal operates in AF mode, the relay terminal simply amplifies the received signal. Therefore, the SIC process is considered at the destination terminal. The OP, EP, AR, ER, and throughput performance metrics are considered in the system performance analysis. It is observed that the optimum power and power allocation coefficients improves the system performance and provide an opportunity to have an information exchange in low SNR regimes compared to non-optimized case. Analytical and asymptotic derivations are verified by means of Monte-Carlo based intensive computer simulations. Derived

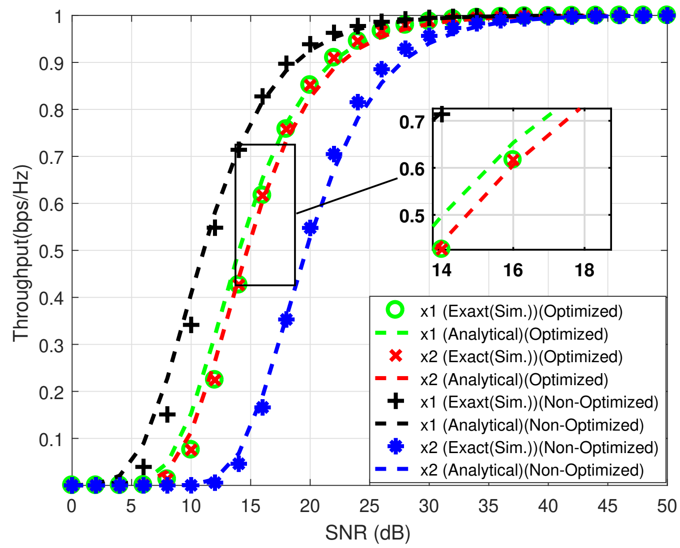

Fig. 10: The optimized and non-optimized throughput performance comparisons of x_1 and x_2.

analytical results can be applied in optimized positioning and operation of wireless sensor nodes in a simple and power-efficient manner.

Appendix

Taking into consideration (8) and utilizing the probability properties following expression can be obtained.

$$
\begin{aligned}
F^{\mathrm{up}}_{\gamma_{\mathrm{X}_1}}(\gamma_{\mathrm{th}}) &= \mathrm{P}_r\Big(\beta_1 \min(\mathrm{A},\mathrm{B}) \le \underbrace{\gamma_{\mathrm{th}}}_{2^{\mathrm{R}}-1}\Big) \\
&= \mathrm{P}_r\left(\beta_1 \min\left(\frac{\gamma_{\mathrm{y}}}{(\beta_1+\beta_2)}, \frac{\gamma_{\mathrm{x}}}{(\gamma_{\mathrm{x}}\beta_2+\gamma_{\mathrm{a}}+2)}\right) \le \gamma_{\mathrm{th}}\right) \\
&= 1-\mathrm{P}_r\left(\gamma_y \ge \frac{\gamma_{\mathrm{th}}(\beta_1+\beta_2)}{\beta_1}, \gamma_x \ge \frac{\gamma_{\mathrm{th}}}{\beta_1}(\gamma_x\beta_2+\gamma_a+2)\right) \\
&= 1-\mathrm{P}_r\left(\gamma_y \ge \frac{\gamma_{th}(\beta_1+\beta_2)}{\beta_1}, \gamma_x \ge \frac{\gamma_{th}(\gamma_a+2)}{(\beta_1-\gamma_{th}\beta_2)}\right) \\
&= 1-\left(\left(1-F_{\gamma_y}\left(\frac{\gamma_{\mathrm{th}}(\beta_1+\beta_2)}{\beta_1}\right)\right)\left(1-F_{\gamma_x}\left(\frac{\gamma_{\mathrm{th}}(\gamma_a+2)}{(\beta_1-\gamma_{\mathrm{th}}\beta_2)}\right)\right)\right) \\
&= 1-\mathbb{E}_{\gamma_a}\left[e^{-\gamma_{\mathrm{th}}\left(\frac{(\beta_1+\beta_2)}{\beta_1\mathrm{P}_s\Omega_g}+\frac{(\gamma_a+2)}{(\beta_1-\gamma_{th}\beta_2)\mathrm{P}_s\Omega_h}\right)}\Bigg|_{\gamma_a}\right] \\
&= 1-e^{-\gamma_{\mathrm{th}}\left(\frac{(\beta_1+\beta_2)}{\beta_1\mathrm{P}_s\Omega_g}+\frac{2}{(\beta_1-\gamma_{th}\beta_2)\mathrm{P}_s\Omega_h}\right)}\int_0^\infty e^{-\gamma_a\left(\frac{\gamma_{\mathrm{th}}}{(\beta_1-\gamma_{th}\beta_2)\mathrm{P}_s\Omega_h}\right)} f\gamma_a(\gamma_a)\,d\gamma_a
\end{aligned}
\tag{34}
$$

Substituting $f\gamma_a(\gamma_a) = \frac{1}{\mathrm{P}_r\Omega_a}e^{-\frac{\gamma_a}{\mathrm{P}_r\Omega_a}}$ [47] into (34) and solving the integral expressions with the help of [39, Eq. (3.310[11])], the final CDF expression can be obtained as in (10). Following the same procedures, $F^{\mathrm{up}}_{\gamma_{\mathrm{X}_2}}(\gamma_{\mathrm{th}})$ can be calculated as in (11). The $R_{x_1}^{\mathrm{up}}$, which is (13), can be rewritten as

$$R_{X_1}^{\mathrm{up}}=\frac{1}{\ln 2}\int_0^{\infty}\mathrm{e}^{-\gamma_{\mathrm{th}}\left(\underbrace{\frac{(\beta_1+\beta_2)}{\beta_1\mathrm{P}_s\Omega_g}}_{\alpha_1}+\frac{2}{(\beta_1-\gamma_{\mathrm{th}}\beta_2)}\underbrace{\frac{1}{\mathrm{P}_s\Omega_h}}_{\alpha_2}\right)}\left(\underbrace{\frac{\mathrm{P}_r\Omega_a}{\mathrm{P}_s\Omega_h}}_{\alpha_3}\frac{\gamma_{\mathrm{th}}}{(\beta_1-\gamma_{\mathrm{th}}\beta_2)}+1\right)^{-1}(1+\gamma_{\mathrm{th}})^{-1}\,\mathrm{d}\gamma_{\mathrm{th}} \tag{35}$$

Let $\gamma_{th}=\frac{\beta_1}{\beta_2}(u+1)$ and $d\gamma_{th}=\frac{\beta_1}{\beta_2}du$. By using these expressions and doing some basic mathematical manipulations, (35) can be rewritten as

$$R_{X_1}^{\mathrm{up}}=\frac{\mathrm{e}^{\left(\frac{2\alpha_2}{\beta_2}-\frac{\beta_1}{\beta_2}\alpha_1\right)}}{\alpha_3\ln 2}\frac{\beta_2}{\beta_1+\beta_2}\int_{-1}^{\infty}\mathrm{e}^{-\frac{\beta_1\alpha_1}{\beta_2}\mathrm{u}+\frac{2\alpha_2}{\beta_2\mathrm{u}}}\left(\frac{-\mathrm{u}}{1+\left(1-\frac{\beta_2}{\alpha_3\beta_1}\right)\mathrm{u}}\right)\left(\frac{1}{1+\frac{\beta_1}{\beta_1+\beta_2}\mathrm{u}}\right)\mathrm{du} \tag{36}$$

Utilizing $e^{\frac{a}{x}}=\sum_{k=0}^{\infty}\frac{a^k}{k!x^k}$ [39] and with the help of [35, Appendix], [35, Eq. 10], and also Meijer-G and Fox-H functions equality, (36) can be rewritten as

$$\begin{aligned}R_{X_1}^{\mathrm{up}}=&-\frac{\mathrm{e}^{\left(\frac{2\alpha_2}{\beta_2}-\frac{\beta_1}{\beta_2}\alpha_1\right)}}{\alpha_3\ln 2}\left(1-\frac{\beta_2}{\alpha_3\beta_1}\right)^{-1}\frac{\beta_2}{\beta_1+\beta_2}\sum_{\mathrm{k}=0}^{\infty}\frac{\left(\frac{2\alpha_2}{\beta_2}\right)^{\mathrm{k}}}{\mathrm{k}!}\times\\&\int_{-1}^{\infty}u^{-k}e^{-\frac{\beta_1\alpha_1}{\beta_2}u}H_{1,1}^{1,1}\left[\left(1-\frac{\beta_2}{\alpha_3\beta_1}\right)u\left|\begin{matrix}(1,1)\\(1,1)\end{matrix}\right.\right]H_{1,1}^{1,1}\left[\frac{\beta_1}{\beta_1+\beta_2}u\left|\begin{matrix}(0,1)\\(0,1)\end{matrix}\right.\right]du\end{aligned} \tag{37}$$

With the help of [35, Eq. 1.1.3], (37) can be represented in terms of the Mellin-Barnes integrals as

$$\begin{aligned}R_{X_1}^{\mathrm{up}}=&-\frac{\mathrm{e}^{\left(\frac{2\alpha_2}{\beta_2}-\frac{\beta_1}{\beta_2}\alpha_1\right)}}{\alpha_3\ln 2}\left(1-\frac{\beta_2}{\alpha_3\beta_1}\right)^{-1}\frac{\beta_2}{\beta_1+\beta_2}\sum_{\mathrm{k}=0}^{\infty}\frac{\left(\frac{2\alpha_2}{\beta_2}\right)^{\mathrm{k}}}{\mathrm{k}!}\int_{-1}^{\infty}\mathrm{u}^{-\mathrm{k}}\mathrm{e}^{-\frac{\beta_1\alpha_1}{\beta_2}\mathrm{u}}\frac{1}{(2\pi\mathrm{j})^2}\left(\int_{\mathrm{c}_1}\int_{\mathrm{c}_2}\Gamma(\mathrm{s})\Gamma(1-\mathrm{s})\,(\Delta\mathrm{u})^{\mathrm{s}}\right.\\&\left.\times\Gamma(-t)\Gamma(1+t)\,(\Lambda u)^t\,dsdt\right)du\end{aligned} \tag{38}$$

where $\Delta=\left(1-\frac{\beta_2}{\alpha_3\beta_1}\right)$ and $\Lambda=\frac{\beta_1}{\beta_1+\beta_2}$. By changing the order of integration, (38) can be rewritten as

$$\begin{aligned}R_{X_1}^{\mathrm{up}}=&-\frac{\mathrm{e}^{\left(\frac{2\alpha_2}{\beta_2}-\frac{\beta_1}{\beta_2}\alpha_1\right)}}{\alpha_3\ln 2}\left(1-\frac{\beta_2}{\alpha_3\beta_1}\right)^{-1}\frac{\beta_2}{\beta_1+\beta_2}\sum_{\mathrm{k}=0}^{\infty}\frac{\left(\frac{2\alpha_2}{\beta_2}\right)^{\mathrm{k}}}{\mathrm{k}!}\frac{1}{(2\pi\mathrm{j})^2}\times\\&\int_{c_1}\int_{c_2}\Gamma(s)\Gamma(1-s)\Delta^s\Gamma(-t)\Gamma(1+t)\Lambda^t\left(\int_{-1}^{\infty}e^{-\frac{\beta_1\alpha_1}{\beta_2}u}u^{s+t-k}du\right)dsdt\end{aligned} \tag{39}$$

The inner integral expression, which is in (39), can be solved by means of [39, Eq. 8.350.2[11]] as $\left(\frac{\alpha_1\beta_1}{\beta_2}\right)^{-(s+t-k+1)}\Gamma\left(s+t-k+1,-\frac{\alpha_1\beta_1}{\beta_2}\right)$. Substituting the integral solution into (39), following expressions can be obtained

$$\begin{aligned}R_{X_1}^{\mathrm{up}}=&-\frac{\mathrm{e}^{\left(\frac{2\alpha_2}{\beta_2}-\frac{\beta_1}{\beta_2}\alpha_1\right)}}{\alpha_3\ln 2}\left(1-\frac{\beta_2}{\alpha_3\beta_1}\right)^{-1}\frac{\beta_2^2}{(\beta_1+\beta_2)\,\alpha_1\beta_1}\sum_{\mathrm{k}=0}^{\infty}\frac{\left(\frac{2\alpha_2}{\beta_2}\right)^{\mathrm{k}}}{\mathrm{k}!}\frac{1}{(2\pi\mathrm{j})^2}\int_{\mathrm{c}_1}\int_{\mathrm{c}_2}\Gamma\left(\mathrm{s}+\mathrm{t}-\mathrm{k}+1,-\frac{\alpha_1\beta_1}{\beta_2}\right)\\&\times\Gamma(s,0)\Gamma(1-s,0)\Gamma(-t,0)\Gamma(1+t,0)\left(\frac{\Delta}{\Upsilon}\right)^s\left(\frac{\Lambda}{\Upsilon}\right)^t dsdt\end{aligned} \tag{40}$$

where $\Upsilon = \frac{\alpha_1\beta_1}{\beta_2}$. Utilizing [37] and [38], (40) can be obtained as in (14). First integral expression in (17) can be solved by dint of [39, Eq. (3.326.2[10])] as $\Gamma\left(\frac{1}{2}\right)$. Regarding the second integral expression in (17), considering the similar procedures as in Appendix B, and using the assumptions, which are $\gamma_{th} = \frac{\beta_1}{\beta_2}(u+1)$ and $d\gamma_{th} = \frac{\beta_1}{\beta_2}du$ and also $\alpha_1 = \frac{(\beta_1+\beta_2)}{\beta_1 \mathrm{P}_s \Omega_g}$, $\alpha_2 = \frac{1}{\mathrm{P}_s \Omega_h}$, $\alpha_3 = \frac{\mathrm{P}_r \Omega_a}{\mathrm{P}_s \Omega_h}$.

$$\bar{P}_{e_{X_1}}^{\text{up}} = \sqrt{\frac{\beta_1}{\beta_2}}\frac{\beta_2}{\alpha_3}\mathrm{e}^{\frac{2\alpha_2}{\beta_2}-\frac{\beta_1}{\beta_2}(1+\alpha_1)}\int_{-1}^{\infty}(\mathrm{u}+1)^{-\frac{1}{2}}\left(\frac{-\mathrm{u}}{1+\left(1-\frac{\beta_2}{\alpha_3}\right)\mathrm{u}}\right)\mathrm{e}^{-\mathrm{u}\left(\frac{\beta_1(\alpha_1+1)}{\beta_2}\right)+\frac{2\alpha_2}{\beta_2 \mathrm{u}}}\mathrm{du} \tag{41}$$

With the help of [35, Appendix] and [34, Eq. 10] and also utilizing the Fox-H and Meijer-G functions equality [48], following expression can be obtained.

$$\bar{P}_{e_{X_1}}^{\text{up}} = \sqrt{\frac{\beta_1}{\beta_2}}\frac{\beta_2}{\alpha_3}\mathrm{e}^{\frac{2\alpha_2}{\beta_2}-\frac{\beta_1}{\beta_2}(1+\alpha_1)}\frac{1}{\sqrt{\pi}}\left(1-\frac{\beta_2}{\alpha_3}\right)^{-1}\int_{-1}^{\infty}\mathrm{e}^{-\mathrm{u}\left(\frac{\beta_1(\alpha_1+1)}{\beta_2}\right)+\frac{2\alpha_2}{\beta_2 \mathrm{u}}}\mathrm{H}_{1,1}^{1,1}\left[\mathrm{u}\left|\begin{matrix}\left(\frac{1}{2},1\right)\\(0,1)\end{matrix}\right.\right]\mathrm{H}_{1,1}^{1,1}\left[\left(1-\frac{\beta_2}{\alpha_3}\right)\mathrm{u}\left|\begin{matrix}(1,1)\\(1,1)\end{matrix}\right.\right]\mathrm{du} \tag{42}$$

With the help of [35, Eq. 1.1.3], (42) can be represented in terms of the Mellin-Barnes types integrals as

$$\begin{aligned}\bar{P}_{e_{X_1}}^{\text{up}} &= \sqrt{\frac{\beta_1}{\beta_2}}\frac{\beta_2}{\alpha_3}\mathrm{e}^{\frac{2\alpha_2}{\beta_2}-\frac{\beta_1}{\beta_2}(1+\alpha_1)}\frac{1}{\sqrt{\pi}}\left(1-\frac{\beta_2}{\alpha_3}\right)^{-1}\times\\ &\int_{-1}^{\infty}e^{-u\left(\frac{\beta_1(\alpha_1+1)}{\beta_2}\right)+\frac{2\alpha_2}{\beta_2 u}}\frac{1}{(2\pi j)^2}\left(\int_{c_1}\int_{c_2}\Gamma(-s)\Gamma(\frac{1}{2}+s)\,(u)^s\,\Gamma(1-t)\Gamma(t)\,(\Psi u)^t\,dsdt\right)du\end{aligned} \tag{43}$$

where $\Psi = \left(1-\frac{\beta_2}{\alpha_3}\right)$. Utilizing $e^{\frac{a}{x}} = \sum_{k=0}^{\infty}\frac{a^k}{k!x^k}$ [39] and by changing the order of integration and solving the inner integral expression with the help of [39, Eq. (8.350.2[11])], following expression can be obtained.

$$\begin{aligned}\bar{P}_{e_{X_1}}^{\text{up}} &= \sqrt{\frac{\beta_1}{\beta_2}}\frac{\beta_2}{\alpha_3}\mathrm{e}^{\frac{2\alpha_2}{\beta_2}-\frac{\beta_1}{\beta_2}(1+\alpha_1)}\frac{1}{\sqrt{\pi}}\left(1-\frac{\beta_2}{\alpha_3}\right)^{-1}\left(\frac{\beta_1(\alpha_1+1)}{\beta_2}\right)^{-1}\sum_{\mathrm{k}=0}^{\infty}\frac{\left(\frac{2\alpha_2}{\beta_2}\right)^{\mathrm{k}}}{\mathrm{k}!}\frac{1}{(2\pi\mathrm{j})^2}\int_{\mathrm{c}_1}\int_{\mathrm{c}_2}\Gamma\Bigg(\mathrm{s}+\mathrm{t}-\mathrm{k}+1,\\ &-\frac{\beta_1(\alpha_1+1)}{\beta_2}\Bigg)\Gamma(-s,0)\Gamma(\frac{1}{2}+s,0)\Gamma(1-t,0)\Gamma(t,0)\left(\frac{1}{\Theta}\right)^s\left(\frac{\Psi}{\Theta}\right)^t dsdt\end{aligned} \tag{44}$$

where $\Theta = \frac{\beta_1(\alpha_1+1)}{\beta_2}$. Utilizing [37] and [38], (44) can be obtained as in (18).

References

[1] Z. Ding *et al.*, "Application of non-orthogonal multiple access in LTE and 5G networks," *IEEE Commun. Magazine*, vol. 55, no. 2, pp. 185–191, February 2017.

[2] N. H. Mahmood, G. Berardinelli, F. M. L. Tavares, and P. Mogensen, "On the potential of full duplex communication in 5g small cell networks," *2015 IEEE 81st Vehicular Technology Conference (VTC Spring)*, pp. 1–5, May 2015.

[3] M. Mohammadi *et al.*, "Full-duplex non-orthogonal multiple access for next generation wireless systems," *IEEE Commun. Mag.*, vol. 57, no. 5, pp. 110–116, 2019.

[4] X. Yue *et al.*, "Exploiting full/half-duplex user relaying in NOMA systems," *IEEE Trans. on Commun.*, vol. PP, no. 99, pp. 1–1, 2017.

[5] L. Zhang *et al.*, "Performance analysis and optimization in downlink noma systems with cooperative full-duplex relaying," *IEEE Journal on Selected Areas in Commun.*, vol. 35, no. 10, pp. 2398–2412, Oct 2017.

[6] Z. Zhang *et al.*, "Full-duplex device-to-device-aided cooperative nonorthogonal multiple access," *IEEE Trans. on Vehic. Techn.*, vol. 66, no. 5, pp. 4467–4471, May 2017.

[7] C. Zhong and Z. Zhang, "Non-orthogonal multiple access with cooperative full-duplex relaying," *IEEE Commun. Let.*, vol. 20, no. 12, pp. 2478–2481, Dec 2016.

[8] J. Men, J. Ge, and C. Zhang, "Performance analysis for downlink relaying aided non-orthogonal multiple access networks with imperfect CSI over Nakagami- m fading," *IEEE Access*, vol. 5, pp. 998–1004, 2017.

[9] J. B. Kim and I. H. Lee, "Capacity analysis of cooperative relaying systems using non-orthogonal multiple access," *IEEE Commun. Let.*, vol. 19, no. 11, pp. 1949–1952, Nov 2015.

[10] X. Liu and X. Wang, "Outage probability and capacity analysis of the collaborative NOMA assisted relaying system in 5G," *2016 IEEE/CIC Intern. Conf. on Commun. in China (ICCC)*, pp. 1–5, July 2016.

[11] M. Xu, F. Ji, M. Wen, and W. Duan, "Novel receiver design for the cooperative relaying system with non-orthogonal multiple access," *IEEE Commun. Let.*, vol. 20, no. 8, pp. 1679–1682, Aug 2016.

[12] J. So and Y. Sung, "Improving non-orthogonal multiple access by forming relaying broadcast channels," *IEEE Commun. Let.*, vol. 20, no. 9, pp. 1816–1819, Sept 2016.

[13] H. Huang *et al.*, "Rate region analysis in a full-duplex-aided cooperative nonorthogonal multiple-access system," *IEEE Access*, vol. 5, pp. 17 869–17 880, 2017.

[14] J. B. Kim and I. H. Lee, "Non-orthogonal multiple access in coordinated direct and relay transmission," *IEEE Commun. Let.*, vol. 19, no. 11, pp. 2037–2040, Nov 2015.

[15] M. S. Elbamby *et al.*, "Resource optimization and power allocation in in-band full duplex (IBFD)-enabled non-orthogonal multiple access networks," *IEEE Journal on Selected Areas in Commun.*, vol. PP, no. 99, pp. 1–1, 2017.

[16] Z. Yang, Z. Ding, Y. Wu, and P. Fan, "Novel relay selection strategies for cooperative NOMA," *IEEE Trans. on Vehic. Techn.*, vol. 66, no. 11, pp. 10 114–10 123, Nov 2017.

[17] X. Liang *et al.*, "Outage performance for cooperative NOMA transmission with an AF relay," *IEEE Commun. Let.*, vol. 21, no. 11, pp. 2428–2431, Nov 2017.

[18] Y. Liu, G. Pan, H. Zhang, and M. Song, "Hybrid decode-forward & amplify-forward relaying with non-orthogonal multiple access," *IEEE Access*, vol. 4, pp. 4912–4921, 2016.

[19] D. Deng *et al.*, "Joint user and relay selection for cooperative NOMA networks," *IEEE Access*, vol. 5, pp. 20 220–20 227, 2017.

[20] S. Lee *et al.*, "Non-orthogonal multiple access schemes with partial relay selection," *IET Commun.*, vol. 11, no. 6, pp. 846–854, 2017.

[21] J. Men, J. Ge, and C. Zhang, "Performance analysis of nonorthogonal multiple access for relaying networks over Nakagami-m fading channels," *IEEE Trans. on Vehic. Techn.*, vol. 66, no. 2, pp. 1200–1208, Feb 2017.

[22] D. Wan *et al.*, "Cooperative NOMA systems with partial channel state information over Nakagami-m fading channels," *IEEE Trans. on Commun.*, vol. PP, no. 99, pp. 1–1, 2017.

[23] X. Yue, Y. Liu, S. Kang, and A. Nallanathan, "Performance analysis of NOMA with fixed gain relaying over Nakagami- m fading channels," *IEEE Access*, vol. 5, pp. 5445–5454, 2017.

[24] Y. Zhang, J. Ge, and E. Serpedin, "Performance analysis of nonorthogonal multiple access for downlink networks with antenna selection over Nakagami-m fading channels," *IEEE Trans. on Vehic. Techn.*, vol. 66, no. 11, pp. 10 590–10 594, Nov 2017.

[25] C. Xue, Q. Zhang, Q. Li, and J. Qin, "Joint power allocation and relay beamforming in nonorthogonal multiple access amplify-and-forward relay networks," *IEEE Trans. on Vehic. Techn.*, vol. 66, no. 8, pp. 7558–7562, Aug 2017.

[26] S. Shabdanov, P. Mitran, and C. Rosenberg, "Achieving optimal throughput in cooperative wireless multihop networks with rate adaptation and continuous power control," *IEEE Trans. on Wireless Commun.*, vol. 13, no. 7, pp. 3880–3891, July 2014.

[27] O. Abbasi and A. Ebrahimi, "Cooperative noma with full-duplex amplify-and-forward relaying," *Transactions on Emerging Telecommun. Techn.*, vol. 29, no. 7, p. e3421, 2018, e3421 ett.3421. [Online]. Available: https://onlinelibrary.wiley.com/doi/abs/10.1002/ett.3421

[28] X. Li *et al.*, "Full-duplex cooperative noma relaying systems with i/q imbalance and imperfect sic," *IEEE Wireless Commun. Letters*, vol. 9, no. 1, pp. 17–20, 2020.

[29] Z. Ding, P. Fan, and H. V. Poor, "On the coexistence between full-duplex and noma," *IEEE Wireless Commun. Letters*, vol. 7, no. 5, pp. 692–695, 2018.

[30] K. Reshma and A. V. Babu, "Cooperative noma system with incremental relaying and energy harvesting: Performance analysis and optimization," *Trans. on Emerging Telecommun. Techn.*, vol. 31, no. 9, p. e4075, 2020. [Online]. Available: https://onlinelibrary.wiley.com/doi/abs/10.1002/ett.4075

[31] M. W. Baidas, E. Alsusa, and K. A. Hamdi, "Joint relay selection and energy-efficient power allocation strategies in energy-harvesting cooperative noma networks," *Trans. on Emerging Telecommun. Techn.*, vol. 30, no. 7, p. e3593, 2019, e3593 ett.3593. [Online]. Available: https://onlinelibrary.wiley.com/doi/abs/10.1002/ett.3593

[32] S. R. Islam, M. Zeng, O. A. Dobre, and K.-S. Kwak, "Nonorthogonal multiple access (noma): How it meets 5g and beyond," pp. 1–28, 2019. [Online]. Available: https://onlinelibrary.wiley.com/doi/abs/10.1002/9781119471509.w5GRef032

[33] S. M. R. Islam, N. Avazov, O. A. Dobre, and K. Kwak, "Power-domain non-orthogonal multiple access (noma) in 5g systems: Potentials and challenges," *IEEE Commun. Surveys Tutorials*, vol. 19, no. 2, pp. 721–742, 2017.

[34] V. S. Adamchik and O. I. Marichev, *The algorithm for calculating integrals of hypergeometric type functions and its realization in REDUCE systems*. Proc. Conf. ISSAC'90, Tokyo, pp. 212–224, 1990.

[35] A. M. Mathai and R. K. Saxena, *The H-function with application in statistics and other disciplines*, 1978.

[36] N. H. Mahmood *et al.*, "Physical-layer security with full-duplex transceivers and multiuser receiver at eve," *IEEE Trans. on Commun.*, vol. 65, no. 10, pp. 4392–4405, Oct 2017.

[37] F. Yilmaz and M. Alouini, "Product of shifted exponential variates and outage capacity of multicarrier systems," *2009 European Wireless Conference*, pp. 282–286, 2009.

[38] A. K. R. Pushpa N. Rathie and L. C. de S. M. Ozelim, "On the distribution of the product and the sum of generalized shifted gamma random variables," *Mathematica Eterna*, vol. 3, no. 6, pp. 421–432, 2013.

[39] I. S. Gradshteyn and I. M. Ryzhik, *Tables of Integrals, Series and Products*. Elsevier Inc., 7th edition, 2007.

[40] S. S. Ikki and S. Aissa, "Performance analysis of two-way amplify-and-forward relaying in the presence of co-channel interferences," *IEEE Trans. on Commun.*, vol. 60, no. 4, pp. 933–939, April 2012.

[41] L. Yang, K. Qaraqe, E. Serpedin, and M. S. Alouini, "Performance analysis of amplify-and-forward two-way relaying with co-channel interference and channel estimation error," *2013 IEEE Wireless Commun. and Netw. Conf. (WCNC)*, pp. 3710–3714, April 2013.

[42] Wolfram, *The Wolfram Functions Site [Online] Available: http://functions.wolfram.com/07.34.21.0081.01*, 2017.

[43] E. Soleimani-Nasab, M. Matthaiou, M. Ardebilipour, and G. K. Karagiannidis, "Two-way AF relaying in the presence of co-channel interference," *IEEE Trans. on Commun.*, vol. 61, no. 8, pp. 3156–3169, August 2013.

[44] T. Nguyen, H. H. K. Duy, H. Nguyen, and M. Voznak, "Throughput analysis in relaying cooperative systems considering time-switching with noma," *2018 41st Intern. Conf. on Telecommun. and Signal Processing (TSP)*, pp. 1–4, July 2018.

[45] Wolfram, *The Wolfram Functions Site [Online] Available: http://functions.wolfram.com/07.34.03.0723.01*, 2019.

[46] L. J. Rodríguez, N. H. Tran, and T. Le-Ngoc, "Performance of full-duplex AF relaying in the presence of residual self-interference," *IEEE Journal on Selected Areas in Commun.*, vol. 32, no. 9, pp. 1752–1764, Sept 2014.

[47] A. Papoulis and U. Pillai, *Probability, random variables and stochastic processes*, 4th ed. McGraw-Hill, 11 2001.

[48] Wolfram, *The Wolfram Functions Site [Online] Available: http://functions.wolfram.com/07.34.26.0008.01*, 2018.